Sliding-Mode Tracking Control of Nonholonomic Wheeled Mobile Robots in Polar Coordinates

Dongkyoung Chwa

***Abstract*—This brief proposes a sliding-mode control method for wheeled-mobile robots in polar coordinates. A new sliding-mode control method is proposed for mobile robots with kinematics in two-dimensional polar coordinates. In the proposed method, two controllers are designed to asymptotically stabilize the tracking errors in position and heading direction, respectively. By combining these controllers together, both asymptotic posture (position and heading direction) stabilization and trajectory tracking are achieved for reference trajectories at global regions except the arbitrary small region around the origin. In particular, constraints on the desired linear and angular velocities as well as the posture of the mobile robot are eliminated unlike the previous studies based on kinematics expressed in polar coordinates. Accordingly, arbitrary trajectories including a circle and a straight line in various forms can be followed even with large initial tracking errors and bounded disturbances. The stability and performance analyzes are performed and also simulations are included to confirm the effectiveness of the proposed scheme.**

***Index Terms*—Polar coordinates, posture stabilization, sliding-mode control, trajectory tracking, wheeled-mobile robots.**

I. Introduction

MUCH research has been done on the tracking control of a mobile robot [1]. Wheeled-mobile robots have nonholonomic constraints since they have restricted mobility in that the wheels roll without slipping. In particular, a linearized mobile robot model is shown to have deficiency in controllability and the linear control method cannot be employed [2]. Thus, nonlinear control for this class of system has been studied extensively.

The representation of the kinematic equations of mobile robot for the trajectory control can be classified into Cartesian coordinates [3]–[11] and polar coordinates [12]–[15]. Although posture of the mobile robot can be readily represented with respect to the target frame by using the polar coordinates, Cartesian coordinate representation is more often adopted due to the possible singular points in polar coordinate representation. In [7] and [8], the global tracking problem with arbitrary initial tracking errors is solved when the desired linear and angular velocities are constrained, which has been recently eliminated in [9]. Although a single controller is designed for both tracking and stabilization in [9], the control parameter should be adjusted depending on the reference trajectories, and the persistently exciting control input should be included. On the other hand, as uncertainties exist in the real mobile robot, adaptive and sliding-mode control theories are employed in [10], [11], and [14] to solve this problem. The tracking errors are just attenuated in [10] and the desired velocities need to be constrained for exact tracking in [11]. In the case of [14], the external disturbances are considered using sliding surface in polar coordinates, but the posture should be constrained and, accordingly, arbitrary trajectories cannot be globally followed. Thus, a control law needs to be developed so that arbitrary trajectory tracking is possible even with large initial tracking errors and disturbances without any constraints on desired velocities.

In this paper, a new sliding-mode control method is proposed for trajectory tracking of a nonholonomic wheeled-mobile robot in polar coordinates. By proposed method, the geometric constraints in [14] is eliminated and both tracking and stabilization problem are solved as in [9]. The global asymptotic stabilization and tracking results are valid for reference trajectories at global regions except the small region around the origin and also the controller is dependent on the type of reference trajectory as in [9]. However, persistently exciting control inputs in [9] are not needed in the proposed control law. In particular, even when tracking a straight line, a circular path, and a path approaching the origin, linear and angular velocities do not vibrate as in [9]. Due to the nonholonomic constraints on the motion, it becomes critical to select the sliding surface so that three tracking errors in position and orientation are reduced using two control inputs. Noting that a proper choice of tracking errors can eliminate the geometric constraints, two sliding surfaces in polar coordinates are chosen in terms of tracking errors in both position and heading direction, where posture constraints are eliminated. Based on these sliding surfaces, two sliding-mode controllers are designed as *positron controller* and *heading direction controller*. One is to guarantee the asymptotic position tracking even with the heading-direction error when the position-tracking errors exist or the reference trajectories are moving. The other is to guarantee the asymptotic heading direction tracking when the position-tracking errors are sufficiently small and the reference trajectory does not move. The stability and performance of each control system are analyzed. By combining these controllers, the global asymptotic performance of both trajectory tracking and posture stabilization can be achieved even with large initial tracking errors in both position and heading direction, which are shown through numerical simulations conducted for various reference trajectories and initial postures of reference trajectory and mobile robot.

II. Dynamics and Kinematics of Wheeled Mobile Robots

In this section, dynamics and kinematics of wheeled-mobile robots are shown under the nonholonomic constraints as in [3],

Manuscript received April 24, 2003. Manuscript received in final form December 2, 2003. Recommended by Associate Editor S. K. Agrawal. This work was supported by Brain Korea 21 Project, Seoul National University, Seoul, Korea.

The author is with the School of Electrical Engineering and Computer Science, Seoul National University, Kwanak, Seoul 151-742, Korea (e-mail: dkchwa@neuro.snu.ac.kr).

Digital Object Identifier 10.1109/TCST.2004.824953

1063-6536/04$20.00 © 2004 IEEE

[4]. The dynamic equations under nonholonomic constraints can be described by Euler–Lagrange formulation [5] as

$$M(q)\ddot{q} + V(q,\dot{q})\dot{q} + G(q) = B(q)\tau + A^T(q)\lambda \tag{1}$$

where $q \in R^n$ is generalized coordinates, $\tau \in R^r$ is a torque control input vector, $\gamma \in R^m$ is a constraint force vector, $M(q) \in R^{n\times n}$ is a symmetric and positive definite inertia matrix, $V(q,\dot{q}) \in R^{n\times n}$ is a centripetal and coriolis matrix, $G(q) \in R^n$ is a gravitation vector, $B(q) \in R^{n\times r}$ is an input transformation matrix, and $A(q) \in R^{m\times n}$ is a matrix related with nonholonomic constraints. In the following, $r = n - m$ is assumed.

The nonholonomic kinematic constraints are described by

$$A(q)\dot{q} = 0 \tag{2}$$

and the following relation can be obtained:

$$A(q)S(q) = 0 \tag{3}$$

where $S(q) \in R^{n\times(n-m)} = R^{n\times r}$ is composed of linearly independent vectors in the null space of $A(q)$. From (2) and (3), $(n-m)$-dimensional vector z exists such that

$$\dot{q} = S(q)z \tag{4}$$

where z corresponds to the internal state variable. Differentiating (4) we have

$$\ddot{q} = S(q)\dot{z} + \dot{S}(q)z. \tag{5}$$

Substitution of (4) and (5) into (1) yields

$$\begin{aligned} M(q)S(q)\dot{z} + \left\{M(q)\dot{S}(q) + V(q,\dot{q})S(q)\right\} z &+ \\ G(q) - A^T(q)\lambda &= B(q)\tau \end{aligned} \tag{6}$$

or

$$\begin{aligned} S^T(q)M(q)S(q)\dot{z} + S^T(q)\left[\left\{M(q)\dot{S}(q) + V(q,\dot{q})S(q)\right\} z \right. &+ \\ \left. G(q)\right] &= S^T(q)B(q)\tau \end{aligned} \tag{7}$$

using $S^T(q)A^T(q) = 0$ in (3). Thus, the dynamic equations are given by

$$H(q)\dot{z} + F(q,z) = \tau \tag{8}$$

where

$$\begin{aligned} H(q) &= \left[S^T(q)B(q)\right]^{-1} S^T(q)M(q)S(q) \\ F(q,z) &= \left[S^T(q)B(q)\right]^{-1} S^T(q) \\ &\quad \times \left[\left\{M(q)\dot{S}(q) + V(q,\dot{q})S(q)\right\} z + G(q)\right]. \end{aligned}$$

Defining variables q and z in (4) as $q^T = [x_c\, y_c\, \theta_c]$ and $z^T = [v_c\, \omega_c]$, a nonholonomic constraint on the rolling motion of the robot wheel without slipping, given by (2), can be expressed as

$$\dot{x}_c \sin\theta_c - \dot{y}_c \cos\theta_c = 0. \tag{9}$$

The kinematic equations in Cartesian coordinates corresponding to (4) is

$$\begin{pmatrix} \dot{x}_c \\ \dot{y}_c \\ \dot{\theta}_c \end{pmatrix} = \begin{pmatrix} v_c\cos\theta_c \\ v_c\sin\theta_c \\ \omega_c \end{pmatrix} \tag{10}$$

where x_c and y_c are position variables, θ_c is a heading direction angle, v_c is a forward linear velocity, ω_c is an angular velocity of the mobile robot. Also, the kinematic equations in polar coordinates become

$$\begin{pmatrix} \dot{\rho}_c \\ \dot{\phi}_c \\ \dot{\theta}_c \end{pmatrix} = \begin{pmatrix} v_c\cos(\phi_c - \theta_c) \\ -\frac{v_c}{\rho_c}\sin(\phi_c - \theta_c) \\ \omega_c \end{pmatrix} \tag{11}$$

where $\rho_c = \sqrt{(x_c^2 + y_c^2)}$ and $\phi_c = \tan^{-1}(y_c/x_c)$. In this case, variables q and z in (4) can be expressed as $q^T = [\rho_c\, \phi_c\, \theta_c]$ and $z^T = [v_c\, \omega_c]$.

III. Sliding-Mode Tracking Control

The control objective is to steer the mobile robot so as to follow the desired trajectory, which can be represented in polar coordinates. Using the expression in (11) a reference trajectory becomes

$$\begin{pmatrix} \dot{\rho}_r \\ \dot{\phi}_r \\ \dot{\theta}_r \end{pmatrix} = \begin{pmatrix} v_r\cos(\phi_r - \theta_r) \\ -\frac{v_r}{\rho_r}\sin(\phi_r - \theta_r) \\ \omega_r \end{pmatrix} \tag{12}$$

for $q_r^T = [\rho_r\, \phi_r\, \theta_r]$ and $z_r^T = [v_r\, \omega_r]$. When ρ_r becomes zero, ϕ_r-equation in (12) cannot be defined. Thus, (12) is valid for $\rho_r \geq \rho_\varepsilon > 0$. In case of $\rho_r < \rho_\varepsilon$, $v_r = \omega_r = 0$ can be substituted into (12) to have $\dot{\rho}_r = \dot{\phi}_r = \dot{\theta}_r = 0$, which results in modeling error. From now on, we will assume for brevity that ρ_c, $\rho_r \geq \rho_\varepsilon > 0$, i.e., (11) and (12) will be considered as actual and reference kinematic equations. Here, ρ_r, ϕ_r, θ_r, and their first- and second-order time derivatives are assumed to be bounded without loss of generality.

When the tracking errors in polar coordinates are chosen as

$$\rho_e = \rho_c - \rho_r, \quad \phi_e = \phi_c - \phi_r, \quad \theta_e = \theta_c - \theta_r \tag{13}$$

the convergence of (13) to zero can be achieved by making the following variables converge to zero:

$$s_\rho = \dot{\rho}_e + k_1\rho_e, \quad s_\phi = \dot{\phi}_e + k_2\phi_e, \quad s_\theta = \dot{\theta}_e + k_3\theta_e \tag{14}$$

where $k_i > 0, i = 1,2,3$. However, three variables in (14) cannot be chosen as the sliding surfaces as these variables cannot be reduced to zero at the same time using only two variables v_c and ω_c.

For this, we modify (11) and (12) as

$$M(\rho_c,\phi_c,\theta_c)\begin{pmatrix} \dot{\rho}_c \\ \dot{\phi}_c \\ \dot{\theta}_c \end{pmatrix} = \begin{pmatrix} v_c \\ \omega_c \end{pmatrix} \tag{15}$$

$$M(\rho_r,\phi_r,\theta_r)\begin{pmatrix} \dot{\rho}_r \\ \dot{\phi}_r \\ \dot{\theta}_r \end{pmatrix} = \begin{pmatrix} v_r \\ \omega_r \end{pmatrix} \tag{16}$$

where

$$M(m_1,m_2,m_3)=\begin{pmatrix}\cos(m_2-m_3) & -m_1\sin(m_2-m_3) & 0\\ \sin(m_2-m_3) & m_1\cos(m_2-m_3) & 1\end{pmatrix}.$$

Based on the above representation, the sliding surface s is chosen for $k_0 > 1$ as

$$s = M(\rho_c,\phi_c,\theta_c)\begin{pmatrix} s_\rho + k_0\mathrm{sgn}(\rho_e)|s_\theta| \\ s_\phi + \frac{k_0}{\rho_c}\mathrm{sgn}(\phi_e)|s_\theta| \\ s_\theta \end{pmatrix}. \tag{17}$$

Remark 1: Even when ρ_c decreases to zero, s is well defined and the resulting controller can be free from the problem of singularity around the origin, as can be seen later in Figs. 3(c) and (d). The proof of Theorem 1 will show that the convergence of s to zero implies that of ρ_e and ϕ_e from (17) or asymptotic position tracking.

Here, the following assumption on disturbances is made as in [14].

Assumption 1: The bounded disturbances τ_d exist in system dynamics (8) as

$$H(q)\dot{z} + F(q,z) + \tau_d = \tau \tag{18}$$

where $\tau_d = H(q)f$, $f = [f_1\ f_2]^T$, $|f_i| \le f_{mi}$, $i = 1{,}2$, $\tau = [\tau_l\ \tau_r]^T$ and is a torque vector for left and right wheels. Also, $H(q)$ and $F(q,z)$ are assumed to be known.

Using the computed-torque method, a torque control input τ can be chosen from (18) as

$$\tau = H(q)\dot{z}_r + F(q,z) + H(q)u \tag{19}$$

and the corresponding control input u is proposed as

$$\begin{aligned} u =& \dot{M}(\rho_c,\phi_c,\theta_c)\begin{pmatrix} -k_1\rho_e + \dot{\rho}_r \\ -k_2\phi_e + \dot{\phi}_r \\ -k_3\theta_e + \dot{\theta}_r \end{pmatrix} \\ &+ M(\rho_c,\phi_c,\theta_c)\begin{pmatrix} -k_1\dot{\rho}_e + \ddot{\rho}_r \\ -k_2\dot{\phi}_e + \ddot{\phi}_r \\ -k_3\dot{\theta}_e + \ddot{\theta}_r \end{pmatrix} \\ &- \dot{M}(\rho_r,\phi_r,\theta_r)\begin{pmatrix} \dot{\rho}_r \\ \dot{\phi}_r \\ \dot{\theta}_r \end{pmatrix} - M(\rho_r,\phi_r,\theta_r)\begin{pmatrix} \ddot{\rho}_r \\ \ddot{\phi}_r \\ \ddot{\theta}_r \end{pmatrix} \\ &- \begin{pmatrix} \frac{d}{dt}\left[k_0\cos(\phi_c-\theta_c)\mathrm{sgn}(\rho_e)|s_\theta| \right. \\ \left. -k_0\sin(\phi_c-\theta_c)\mathrm{sgn}(\phi_e)|s_\theta|\right] \\ \frac{d}{dt}\left[k_0\sin(\phi_c-\theta_c)\mathrm{sgn}(\rho_e)|s_\theta| \right. \\ \left. +k_0\cos(\phi_c-\theta_c)\mathrm{sgn}(\phi_e)|s_\theta|\right] \end{pmatrix} \\ &- Qs - P\mathrm{sgn}(s) \end{aligned} \tag{20}$$

where $Q = \mathrm{diag}(q_1,q_2) > 0$, $P = P_0 + P_f = \mathrm{diag}(p_1,p_2)$, $P_0 = \mathrm{diag}(\eta_1,\eta_2) > 0$, $P_f = \mathrm{diag}(f_{m1},f_{m2}) > 0$, $\mathrm{sgn}(s) = [\mathrm{sgn}(s_1)\ \mathrm{sgn}(s_2)]^T$. Then, the control system satisfies the property in the following theorem.

Theorem 1 (Position Controller): Under Assumption 1, control inputs (19), (20) stabilize the sliding surface (17) for $\rho_r \ge \rho_\varepsilon > 0$. Then, position-tracking errors converge to zero and heading-direction error is bounded.

Proof: (19) reduces (18) into

$$\dot{z} + f = \dot{z}_r + u \tag{21}$$

and this, in turn, becomes

$$\begin{pmatrix} \dot{v}_c - \dot{v}_r \\ \dot{\omega}_c - \dot{\omega}_r \end{pmatrix} = \begin{pmatrix} u_1 \\ u_2 \end{pmatrix} - \begin{pmatrix} f_1 \\ f_2 \end{pmatrix}. \tag{22}$$

Now, the difference between (15) and (16) can be arranged as

$$\begin{aligned} &M(\rho_c,\phi_c,\theta_c)\begin{pmatrix} \dot{\rho}_e \\ \dot{\phi}_e \\ \dot{\theta}_e \end{pmatrix} + M(\rho_c,\phi_c,\theta_c)\begin{pmatrix} \dot{\rho}_r \\ \dot{\phi}_r \\ \dot{\theta}_r \end{pmatrix} - \\ &\qquad M(\rho_r,\phi_r,\theta_r)\begin{pmatrix} \dot{\rho}_r \\ \dot{\phi}_r \\ \dot{\theta}_r \end{pmatrix} = \begin{pmatrix} v_c - v_r \\ \omega_c - \omega_r \end{pmatrix} \end{aligned} \tag{23}$$

and further as

$$\begin{aligned} &s + M(\rho_c,\phi_c,\theta_c)\begin{pmatrix} -k_1\rho_e + \dot{\rho}_r \\ -k_2\phi_e + \dot{\phi}_r \\ -k_3\theta_e + \dot{\theta}_r \end{pmatrix} \\ &- \begin{pmatrix} k_0\cos(\phi_c-\theta_c)\mathrm{sgn}(\rho_e)|s_\theta| \\ -k_0\sin(\phi_c-\theta_c)\mathrm{sgn}(\phi_e)|s_\theta| \\ k_0\sin(\phi_c-\theta_c)\mathrm{sgn}(\rho_e)|s_\theta| \\ +k_0\cos(\phi_c-\theta_c)\mathrm{sgn}(\phi_e)|s_\theta| \end{pmatrix} \\ &- M(\rho_r,\phi_r,\theta_r)\begin{pmatrix} \dot{\rho}_r \\ \dot{\phi}_r \\ \dot{\theta}_r \end{pmatrix} = \begin{pmatrix} v_c - v_r \\ \omega_c - \omega_r \end{pmatrix}. \end{aligned} \tag{24}$$

Substitution of (22) into the time derivative of (24) gives

$$\begin{aligned} \dot{s} =& \begin{pmatrix} u_1 \\ u_2 \end{pmatrix} - \begin{pmatrix} f_1 \\ f_2 \end{pmatrix} - \dot{M}(\rho_c,\phi_c,\theta_c)\begin{pmatrix} -k_1\rho_e + \dot{\rho}_r \\ -k_2\phi_e + \dot{\phi}_r \\ -k_3\theta_e + \dot{\theta}_r \end{pmatrix} \\ &- M(\rho_c,\phi_c,\theta_c)\begin{pmatrix} -k_1\dot{\rho}_e + \ddot{\rho}_r \\ -k_2\dot{\phi}_e + \ddot{\phi}_r \\ -k_3\dot{\theta}_e + \ddot{\theta}_r \end{pmatrix} \\ &+ M(\rho_r,\phi_r,\theta_r)\begin{pmatrix} \dot{\rho}_r \\ \dot{\phi}_r \\ \dot{\theta}_r \end{pmatrix} + M(\rho_r,\phi_r,\theta_r)\begin{pmatrix} \ddot{\rho}_r \\ \ddot{\phi}_r \\ \ddot{\theta}_r \end{pmatrix} \\ &+ \begin{pmatrix} \frac{d}{dt}\left[k_0\cos(\phi_c-\theta_c)\mathrm{sgn}(\rho_e)|s_\theta| \right. \\ \left. -k_0\sin(\phi_c-\theta_c)\mathrm{sgn}(\phi_e)|s_\theta|\right] \\ \frac{d}{dt}\left[k_0\sin(\phi_c-\theta_c)\mathrm{sgn}(\rho_e)|s_\theta| \right. \\ \left. +k_0\cos(\phi_c-\theta_c)\mathrm{sgn}(\phi_e)|s_\theta|\right] \end{pmatrix} \end{aligned} \tag{25}$$

which becomes, by the control input (20)

$$\dot{s} = -Qs - P\mathrm{sgn}(s) - f. \tag{26}$$

Choosing Lyapunov functions as

$$V = \frac{1}{2}s^T s \tag{27}$$

and taking the time derivative, we have

$$\begin{aligned} \dot{V} &= s^T\dot{s} \\ &= -s^TQs - s^T\{P\mathrm{sgn}(s) + f\} \\ &= -s^TQs - s^T\{P_f\mathrm{sgn}(s) + f\} - s^TP_0\mathrm{sgn}(s) \\ &\le -s^TQs - \eta_1|s_1| - \eta_2|s_2|. \end{aligned} \tag{28}$$

Thus, V is bounded for all time, and accordingly, $s \in L_\infty \cap L_2$. In addition, we also have $\dot{s} \in L_\infty$ from (26). Thus, Bar-

TABLE I
PROPOSED CONTROL METHOD FOR TRACKING AND STABILIZATION

	Operating condition	Control law	Sliding surface
Position controller ($v_r \geq 0$)	Position tracking errors exist or position of reference trajectory changes	(19), (20)	(17)
Position controller ($v_r < 0$)	Position tracking errors exist or position of reference trajectory changes	(19), (33)	(32)
Heading direction controller	Position tracking errors are sufficiently small and position of reference trajectory does not change	(19), (35)	(34)

TABLE II
INITIAL CONDITIONS ON VELOCITIES AND POSTURE OF REFERENCE AND MOBILE ROBOT ($v_r(\mathrm{m/s})$: FORWARD LINEAR VELOCITY, $\omega_r(\mathrm{rad/s})$: ANGULAR VELOCITY)

	Operating condition		Reference initial posture ($[\rho_r(0), \phi_r(0), \theta_r(0)]$) ($m, rad, rad$)	Robot initial posture ($[\rho_c(0), \phi_c(0), \theta_c(0)]$) ($m, rad, rad$)
	v_r	ω_r		
Scenario 1	5	0	[1, pi/4, pi/4]	[27.3, 2.38, -0.38]
Scenario 2	0	0	[20, 0, pi/2]	[37.3, 2.38, -0.38]
Scenario 3	5	-0.1	[1, pi/4, pi/2]	[7.3, 2.38, -0.38]
Scenario 4	-12	0.8	[35, pi/4, -pi/4]	[37.3, 2.38, -0.38]
Scenario 5	5	0	[30, pi/4, pi/4]	[17.3, 2.38, -0.38]
Scenario 6	4	0	[25, pi/2, 0]	[0, 0, 0]

balat's lemma guarantees the asymptotic convergence of s to zero. Then, from (17) we have

$$\begin{aligned}\begin{pmatrix} s_\rho \\ s_\phi \end{pmatrix} &= \begin{pmatrix} \cos(\phi_c-\theta_c) & -\rho_c\sin(\phi_c-\theta_c) \\ \sin(\phi_c-\theta_c) & \rho_c\cos(\phi_c-\theta_c) \end{pmatrix}^{-1} \begin{pmatrix} 0 \\ -s_\theta \end{pmatrix} \\ &\quad + \begin{pmatrix} -k_0\mathrm{sgn}(\rho_e)|s_\theta| \\ -\frac{k_0}{\rho_c}\mathrm{sgn}(\phi_e)|s_\theta| \end{pmatrix} \\ &= \begin{pmatrix} -\sin(\phi_c-\theta_c)s_\theta - k_0\mathrm{sgn}(\rho_e)|s_\theta| \\ \frac{-1}{\rho_c}\cos(\phi_c-\theta_c)s_\theta - \frac{k_0}{\rho_c}\mathrm{sgn}(\phi_e)|s_\theta| \end{pmatrix}. \end{aligned} \tag{29}$$

From (29), it can be shown that ρ_e and ϕ_e converge to zero, thus, ρ_c becomes bounded. Since s is bounded, the second row of (17) becomes

$$\begin{aligned}&\sin(\phi_c-\theta_c)\left(s_\rho + k_0\mathrm{sgn}(\rho_e)|s_\theta|\right) \\ &\quad + \cos(\phi_c-\theta_c)\left(\rho_c s_\phi + k_0\mathrm{sgn}(\phi_e)|s_\theta|\right) + s_\theta \\ &\quad = \sin(\phi_c-\theta_c)(\dot\rho_e + k_1\rho_e) \\ &\qquad + \rho_c\cos(\phi_c-\theta_c)(\dot\phi_e + k_2\phi_e) \\ &\qquad + k_0\sin(\phi_c-\theta_c)\mathrm{sgn}(\rho_e)|s_\theta| \\ &\qquad + k_0\cos(\phi_c-\theta_c)\mathrm{sgn}(\phi_e)|s_\theta| + s_\theta \\ &\quad = \sin(\phi_c-\theta_c)(-\dot\rho_r + k_1\rho_e) \\ &\qquad + \rho_c\cos(\phi_c-\theta_c)(-\dot\phi_r + k_2\phi_e) \\ &\qquad + k_0\sin(\phi_c-\theta_c)\mathrm{sgn}(\rho_e)|s_\theta| \\ &\qquad + k_0\cos(\phi_c-\theta_c)\mathrm{sgn}(\phi_e)|s_\theta| + s_\theta \end{aligned} \tag{30}$$

which is also bounded. In the second equality of (30), $\dot\rho_c\sin(\phi_c - \theta_c) + \dot\theta_c\rho_c\cos(\phi_c - \theta_c) = 0$ is used from (11). Since ρ_c, $\dot\rho_r$, ρ_e, $\dot\phi_r$, and ϕ_e are bounded, $\sin(\phi_c-\theta_c)(-\dot\rho_r + k_1\rho_e) + \rho_c\cos(\phi_c-\theta_c)(-\dot\phi_r + k_2\phi_e)$ and, accordingly, s_0 become bounded from (30). Thus, heading direction tracking error is bounded. (Q.E.D.)

The convergence of the position-tracking errors to zero in Theorem 1 is not enough when the reference trajectory moves either forward or backward, since the mobile robot can follow in the opposite direction; that is, θ_e can be asymptotically 0 or π.

In the following, we will show that θ_e converges to zero and π for $v_r \geq 0$ and $v_r < 0$, respectively. Control input (20) is assumed to be $u = -Qs$ or more simply $u = -s$ where k_3, position-tracking errors, disturbance, and signum terms are ignored for simple analysis. This is possible only when Q and k_3 are, respectively, large and small in case of *position controllers* such that $-Qs$ term in the control input is more critical than other terms; Q and k_3 are selected as such for simulations in the next section. Also, it is enough to analyze the convergence of θ_e to either zero or π after position tracking is achieved ($\rho_e = \phi_e = 0$).

Now, the following equation can be considered instead of (22) in this analysis

$$\begin{aligned}\begin{pmatrix} \dot v_c - \dot v_r \\ \dot\omega_c - \dot\omega_r \end{pmatrix} &= -M(\rho_c, \phi_c, \theta_c)\begin{pmatrix} \dot\rho_e \\ \dot\phi_e \\ \dot\theta_e \end{pmatrix} \\ &= -\begin{pmatrix} v_c \\ \omega_c \end{pmatrix} + M(\rho_c, \phi_c, \theta_c)\begin{pmatrix} \dot\rho_r \\ \dot\phi_r \\ \dot\theta_r \end{pmatrix} \\ &= -\begin{pmatrix} v_c \\ \omega_c \end{pmatrix} + \begin{pmatrix} 0 \\ \omega_r \end{pmatrix} \\ &\quad + \begin{pmatrix} \cos(\phi_c-\theta_c)\cos(\phi_r-\theta_r) \\ \quad + \frac{\rho_c}{\rho_r}\sin(\phi_c-\theta_c)\sin(\phi_r-\theta_r) \\ \sin(\phi_c-\theta_c)\cos(\phi_r-\theta_r) \\ \quad - \frac{\rho_c}{\rho_r}\cos(\phi_c-\theta_c)\sin(\phi_r-\theta_r) \end{pmatrix} v_r \\ &= -\begin{pmatrix} v_c \\ \omega_c \end{pmatrix} + \begin{pmatrix} \cos(\theta_e) \\ -\sin(\theta_e) \end{pmatrix} v_r + \begin{pmatrix} 0 \\ \omega_r \end{pmatrix}. \end{aligned} \tag{31}$$

The second row of (31) becomes $\ddot\theta_e + \dot\theta_e + v_r\sin(\theta_e) = 0$ or $\ddot\theta_e + \dot\theta_e - v_r\sin(\theta_e - \pi) = 0$. When $v_r \geq 0$, $\ddot\theta_e + \dot\theta_e + |v_r|\sin(\theta_e) = 0$ or $\ddot\theta_e + \dot\theta_e - |v_r|\sin(\theta_e - \pi) = 0$. Suppose that θ_e is near zero, then, first equation almost becomes $\ddot\theta_e + \dot\theta_e + |v_r|\theta_e = 0$ and θ_e remains stable near zero from Lyapunov analysis of linear-time varying systems [16]. But, when θ_e is near π, second equation almost becomes $\ddot\theta_e + \dot\theta_e - |v_r|(\theta_e - \pi) = 0$, which can have unstable equilibrium near π. This shows that θ_e converges to zero when $v_r \geq 0$. Similarly, θ_e can be shown to converge to π when $v_r < 0$.

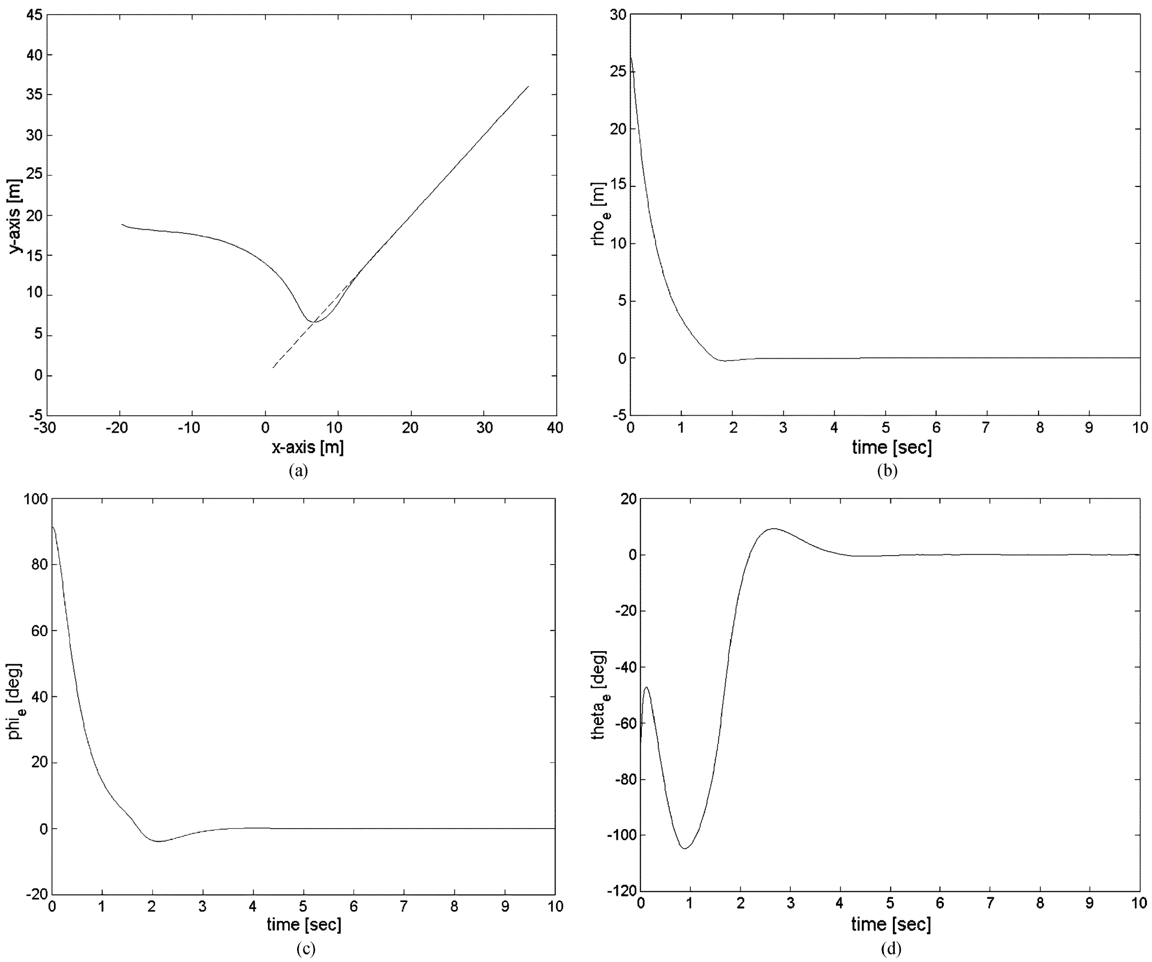

Fig. 1. Trajectory tracking performance of the proposed controller (Scenario 1). (a) $x-y$ plot (dashed: reference, solid: actual model). (b) Tracking error (ρ_e). (c) Tracking error (ϕ_e). (d) Tracking error (θ_e).

Thus, the sliding surface (17) and control law (20) is effective for $v_r \geq 0$. For $v_r < 0$, it can be similarly shown that the following sliding surface and control input guarantee the asymptotic position tracking and the convergence of θ_e to zero.

$$s = N(\rho_c, \phi_c, \theta_c) \begin{pmatrix} s_\rho + k_0 \mathrm{sgn}(\rho_e)|s_\theta| \\ s_\phi + \frac{k_0}{\rho_c}\mathrm{sgn}(\phi_e)|s_\theta| \\ s_\theta \end{pmatrix} \tag{32}$$

$$\begin{aligned} u =& \dot{N}(\rho_c, \phi_c, \theta_c) \begin{pmatrix} -k_1\rho_e + \dot{\rho}_r \\ -k_2\phi_e + \dot{\phi}_r \\ -k_3\theta_e + \dot{\theta}_r \end{pmatrix} \\ &+ N(\rho_c, \phi_c, \theta_c) \begin{pmatrix} -k_1\dot{\rho}_e + \ddot{\rho}_r \\ -k_2\dot{\phi}_e + \ddot{\phi}_r \\ -k_3\dot{\theta}_e + \ddot{\theta}_r \end{pmatrix} \\ &- \dot{N}(\rho_r, \phi_r, \theta_r) \begin{pmatrix} \dot{\rho}_r \\ \dot{\phi}_r \\ \dot{\theta}_r \end{pmatrix} - N(\rho_r, \phi_r, \theta_r) \begin{pmatrix} \ddot{\rho}_r \\ \ddot{\phi}_r \\ \ddot{\theta}_r \end{pmatrix} \\ &- \begin{pmatrix} \frac{d}{dt}\left[k_0 \cos(\phi_c - \theta_c)\mathrm{sgn}(\rho_e)|s_\theta| \right. \\ \left. \quad -k_0 \sin(\phi_c - \theta_c)\mathrm{sgn}(\phi_e)|s_\theta|\right] \\ \frac{d}{dt}\left[-k_0 \sin(\phi_c - \theta_c)\mathrm{sgn}(\rho_e)|s_\theta| \right. \\ \left. \quad -k_0 \cos(\phi_c - \theta_c)\mathrm{sgn}(\phi_e)|s_\theta|\right] \end{pmatrix} \\ &- Qs - P\mathrm{sgn}(s). \end{aligned} \tag{33}$$

where

$$N(m_1, m_2, m_3) = \begin{pmatrix} \cos(m_2 - m_3) & -m_1 \sin(m_2 - m_3) & 0 \\ -\sin(m_2 - m_3) & -m_1 \cos(m_2 - m_3) & 1 \end{pmatrix}.$$

When the reference trajectory does not change its position, the heading direction tracking error is not ensured to be zero by the above *position controller*, and thus another *heading direction controller* is needed. This controller needs to become active when the position-tracking errors become sufficiently small by *position controller* and the position of reference trajectory does not change. Using the sliding surface

$$s = [0 \quad s_\theta]^T \tag{34}$$

instead of (17) or (32), the control input u can be similarly designed starting with (22) as

$$u = \left[0 \quad -k_3\dot{\theta}_e - Q_2 s_\theta - P_2 \mathrm{sgn}(s_\theta)\right]^T. \tag{35}$$

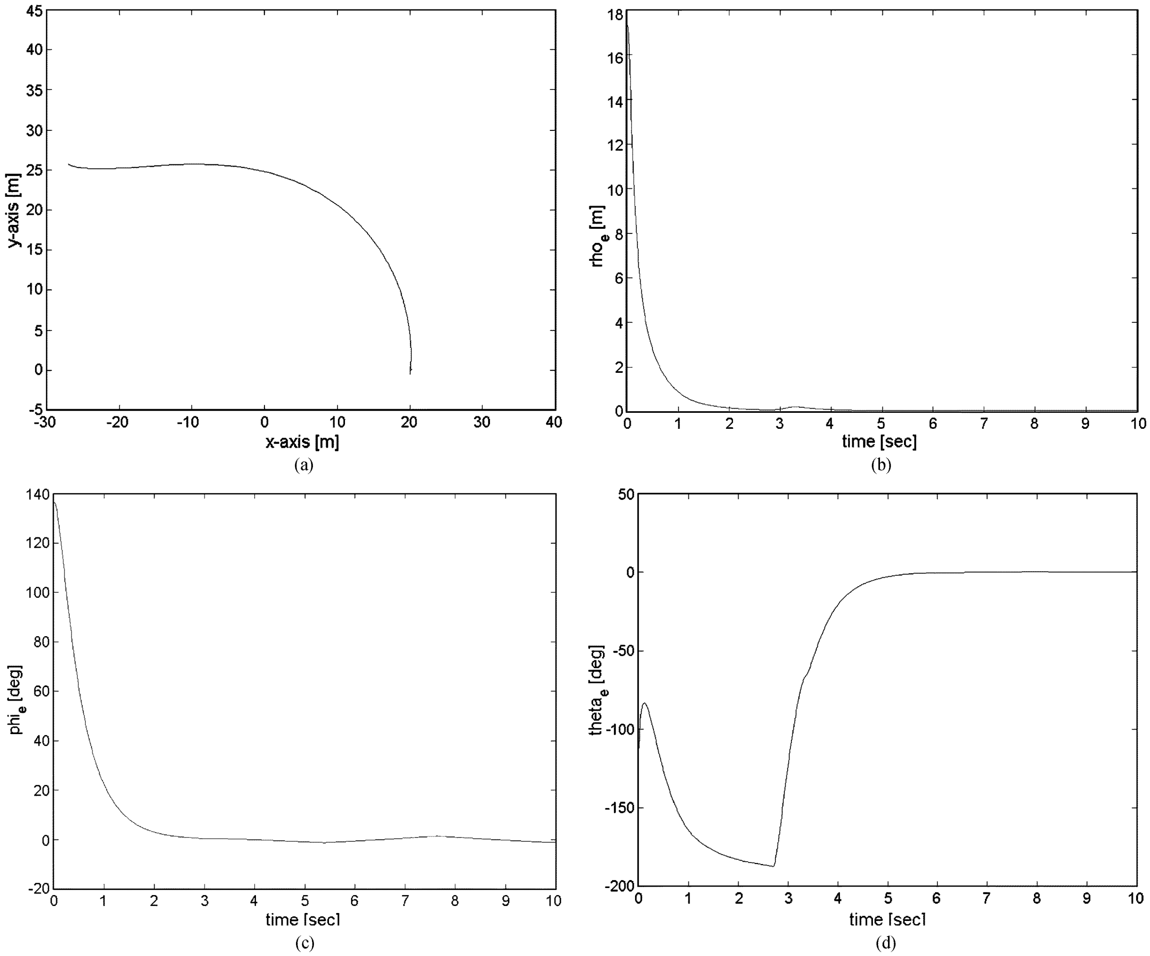

Fig. 2. Trajectory tracking performance of the proposed controller (Scenario 2). (a) $x - y$ plot (dashed: reference, solid: actual model). (b) Tracking error (ρ_e). (c) Tracking error (ϕ_e). (d) Tracking error (θ_e).

Then, as in the proof of Theorem 1, θ_e converges to zero. The overall control scheme for both tracking and stabilization is summarized in Table I.

Remark 2: When saturation functions are used in control inputs (20), (33), (35) and sliding surfaces (17), (32) instead of signum functions, the asymptotic performance is not ensured when the heading-direction error exists. However, the boundedness of the posture-tracking errors can be easily shown.

Remark 3: Unlike the result in [14], constraints on the heading angle of the robot and the angle coordinate, given by $||\phi_c(t) - \theta_c(t)| - (2m+1)(\pi/2)| \geq \alpha$ where $m = 0$ or 1 and α is a positive constant, are not required here. Also, unlike the results in [7], [8], the asymptotic stabilization and tracking performance is possible in Theorem 1 without requiring v_r and ω_r to be zero.

IV. Simulation Results

In this section, simulation results on the wheeled-mobile robot using the proposed method in Table I are presented. The actual and reference kinematics are given by (11) and (12) for $\rho_c, \rho_r \geq \rho_e > 0$, and $\dot{\rho}_c = \dot{\phi}_c = \dot{\theta}_c = \dot{\rho}_r = \dot{\phi}_r = \dot{\theta}_r = 0$ for $\rho_c, \rho_r < \rho_\varepsilon$ where $\rho_\varepsilon = 0.01$; (22) is used instead of (18) for dynamics, which is valid due to the computed-torque control (19). Design parameters of (17), (20), (32), and (33) are $k_0 = 1.1$, $k_1 = k_2 = 2$, $k_3 = 0.002$ while that of (34) and (35) is $k_3 = 2$; $P_1 = P_2 = 1$ and $Q_1 = Q_2 = 10$ in both cases. The signum functions in the control inputs (20), (33), (35), and sliding surfaces (17) and (32) are replaced by saturation functions to reduce the chattering phenomenon. Also, input disturbances are chosen to be Gaussian random noises with mean 0 and variance 0.5 and the upper bounds of disturbances are assumed as $f_{m1} = f_{m2} = 0.5(N)$.

The reference trajectory is generated using the reference model (12), depending on the reference velocities v_r and ω_r, and the initial errors of position and heading direction are assumed to exist as several scenarios in Table II. Here, the reference trajectories of each scenario are: 1) a straight line; 2) a point outside the origin; 3) a curve; 4) a circle; 5) a path toward the origin; and 6) a straight line with initial robot position at origin.

Fig. 1 shows the results for Scenario 1, where it is shown that a straight line can be exactly followed as posture-tracking errors converge to zero as in Fig. 1(b), (c), and (d). Also, the linear and angular velocities do not contain chattering phenomenon, which are omitted here.

Fig. 2, for point stabilization in Scenario 2, shows that the position tracking is achieved first and then the heading direction

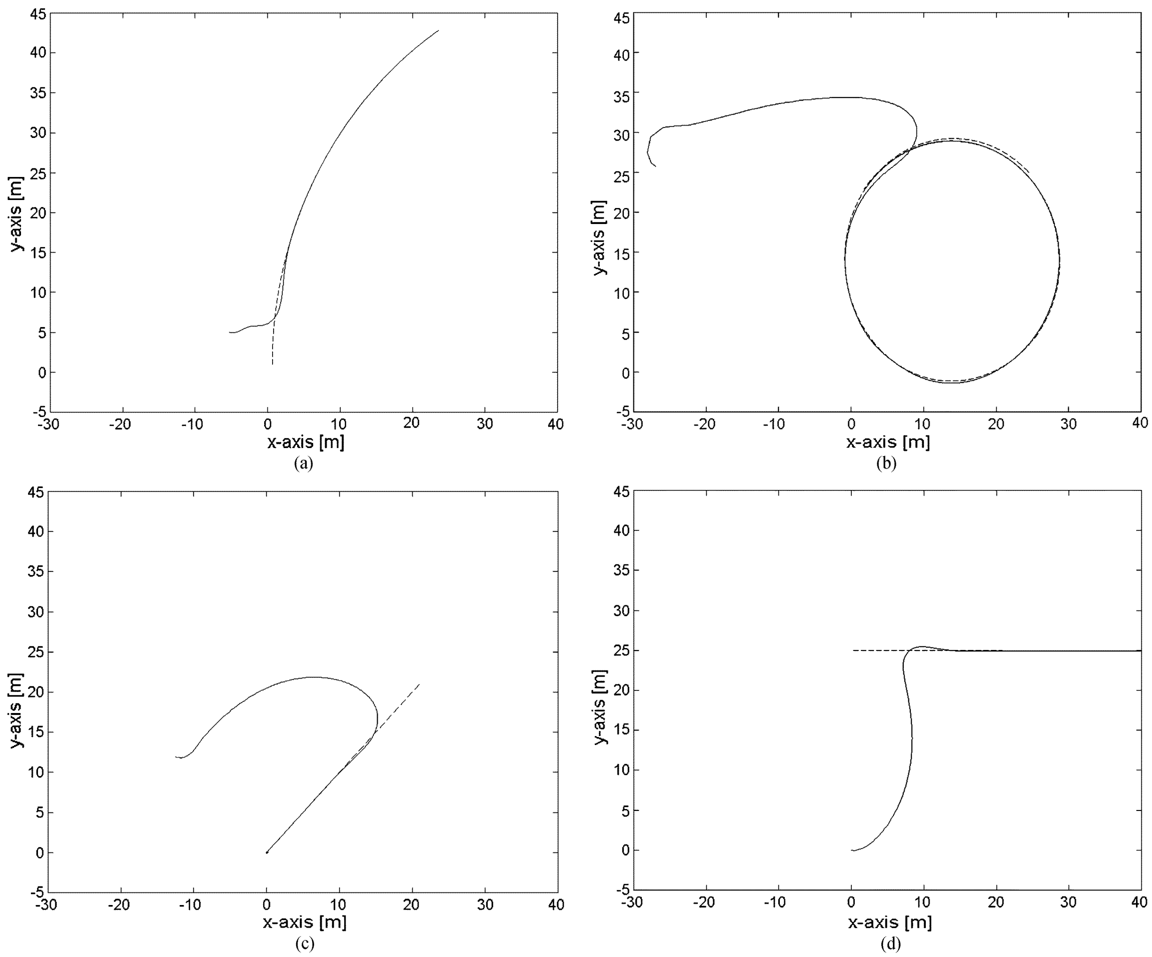

Fig. 3. $x - y$ plot of the mobile robot using the proposed controller (dashed: reference, solid: actual model). (a) Scenario 3. (b) Scenario 4. (c) Scenario 5. (d) Scenario 6.

tracking is achieved. In Fig. 2(b) and (c), position tracking is achieved by *position controller*. When the position tracking error becomes sufficiently small and the reference trajectory does not change its position, *heading direction controller* becomes active to reduce the heading-direction error as in Fig. 2(d).

Fig. 3 shows that tracking performance for reference trajectories in Scenarios 3 through 6 are satisfactory. The tracking errors in these cases also converge to zero, which are omitted here. In particular, the achieved linear velocity follows the negative reference linear velocity in Scenario 4. Since the reference trajectory in polar coordinates cannot be defined at the origin, the distance from the origin becomes sufficiently small in Fig. 3(c). In Fig. 3(d), although the initial position of the mobile robot is the origin in Scenario 6, the asymptotic posture tracking is possible.

V. Conclusion

In this paper, a new sliding-mode control method is proposed for tracking and stabilization of nonholonomic wheeled-mobile robots in polar coordinates. Global asymptotic stabilization and tracking result, for arbitrary trajectories except at the small region around the origin, are obtained without any restriction on the desired velocities. These are also demonstrated in numerical simulations, for reference trajectories including circles and straight lines with various initial conditions. To the best of author's knowledge, similar results could not be obtained in the previous mobile robot control system based on kinematics in polar coordinates. Since the input constraints exist in the actuator, the control method considering the actuator saturation may be necessary in actual implementation, which can be pursued as a further study.

Acknowledgment

The author would like to thank P. Kim for his assistance in conducting the simulation.

References

[1] I. Kolmanovsky and N. H. McClamroch, "Developments in nonholonomic control problems," *IEEE Control Syst. Mag.*, vol. 15, pp. 20–36, Dec. 1995.

[2] R. W. Brockett, "Asymptotic stability and feedback linearization," in *Differential Geometric Control Theory*, R. W. Brockett, R. S. Millman, and H. J. Sussman, Eds. Cambridge, MA: Birkhauser, 1983, pp. 181–191.

[3] Y. Kanayama, Y. Kimura, F. Miyazaki, and T. Noguchi, "A stable tracking control method for an autonomous mobile robot," in *Proc. IEEE Int. Conf. Robotics and Automation*, Cincinnati, OH, 1990, pp. 384–389.

[4] C. Canudas de Wit and O. J. Sordalen, “Exponential stabilization of mobile robot with nonholonomic constraints,” *IEEE Trans. Automat. Contr.*, vol. 37, pp. 1791–1797, Nov. 1992.
[5] C. Samson, “Control of chained system application to path following and time-varying point-stabilization of mobile robots,” *IEEE Trans. Automat. Contr.*, vol. 40, pp. 64–77, Jan. 1995.
[6] G. Campion, B. d'Andrea-Nobel, and G. Bastin, “Controllability and state feedback stabilizability of nonholonomic mechanical systems,” in *Advanced Robotics Control*, C. Canudas de Wit, Ed. New York: Springer-Verlag, 1991, pp. 106–124.
[7] Z.-P. Jiang and H. Nijmeijer, “Tracking control of mobile robots: a case study in backstepping,” *Automatica*, vol. 33, no. 7, pp. 1393–1399, 1997.
[8] Z.-P. Jiang, E. Lefeber, and H. Nijmeijer, “Saturated stabilization and tracking of a nonholonomic mobile robot,” *Syst. Control Lett.*, vol. 42, pp. 327–332, 2001.
[9] T.-C. Lee, K.-T. Song, C.-H. Lee, and C.-C. Teng, “Tracking control of unicycle-modeled mobile robots using a saturation feedback controller,” *IEEE Trans. Contr. Syst. Technol.*, vol. 9, pp. 305–318, Mar. 2001.
[10] Y.-C. Chang and B.-S. Chen, “Adaptive tracking control design of nonholonomic mechanical systems,” in *Proc. Conf. Decision and Control*, Kobe, Japan, Dec. 1996, pp. 4739–4744.
[11] T. Fukao, H. Nakagawa, and N. Adachi, “Adaptive tracking control of a nonholonomic mobile robot,” *IEEE Trans. Robot. Automat.*, vol. 16, pp. 609–615, Oct. 2000.
[12] M. Aicardi, G. Casalino, A. Bicchi, and A. Balestrino, “Closed loop steering of unicycle-like vehicles via Lyapunov techniques,” *IEEE Robot. Automat. Mag.*, pp. 27–35, Mar. 1995.
[13] K. Park, H. Chung, and J. G. Lee, “Point stabilization of mobile robots via state-space exact feedback linearization,” *Robot. Comput.-Integr. Manuf.*, vol. 16, pp. 353–363, 2000.
[14] J.-M. Yang and J.-H. Kim, “Sliding mode control for trajectory tracking of nonholonomic wheeled mobile robots,” *IEEE Trans. Robot. Automat.*, vol. 15, no. 3, pp. 578–587, 1999.
[15] S.-O. Lee, Y.-J. Cho, M. Hwang-Bo, B.-J. You, and S.-R. Oh, “A stable target-tracking control for unicycle mobile robots,” in *Proc. 2000 IEEE/RSJ Int. Conf. Intelligent Robots and Systems*, Takamatsu, Japan, 2000, pp. 1822–1827.
[16] J.-J. E. Slotine and W. Li, *Applied Nonlinear Control*. Englewood Cliffs, NJ: Prentice-Hall, 1991.